Brick finding efficiency : Monte Carlo comparisons between several scintillating tracker options

G. Moret, L. Chaussard, Y. Déclais, S. Katsanevas, P. Jonsson, J. Marteau

OPERA Note 23 May, 2001

Brick finding efficiency : Monte-Carlo comparisons between several scintillating tracker options

G. Moret, L.Chaussard, Y Déclais,
S. Katsanevas, P. Jonsson, J. Marteau
moret@ipnl.in2p3.fr

Institut de Physique Nucléaire de Lyon
Université Claude Bernard Lyon I
F-69622 Villeurbanne cedex

Abstract :

We have simulated plastic and liquid scintillators. The brick finding efficiency for DIS and QE events has been computed for the two options with different cell sizes. We also perform a comparison between a readout at two ends and a readout at one end with a mirror at the other end. The effects of the reflectivity of the mirror and of the fiber attenuation length have been investigated.

1 Introduction

The target tracker of OPERA consists of 24 scintillator walls. The baseline design foresees plastic scintillator strips. An alternative option consists of liquid scintillator strips. In each case, two sizes have been simulated for the scintillator strips. Performances in term of brick finding efficiency and of energy resolution (with a barycentric method) for each option have been compared.

We have simulated and compared :

- plastic and liquid scintillator,
- cell of 1×1 cm^2 and cell of 1×2.6 cm^2,
- one end readout versus two end readout,
- the effect of the attenuation length,
- the effect of a clear fiber.

This note is organized as follows : Section 2 describes the simulation. Section 3 is dedicated to the plastic scintillator and Section 4 is dedicated to the liquid scintillator. Section 5 gives a comparison between one end readout and two ends readout and the effect of the characteristics of the mirror on the brick finding efficiency. Section 6 is dedicated to the study of a clear fiber continuation to the photo-detector.

2 The simulation tools

The simulation is done with the AIDA (v4r2) and ADORE (v3r1) packages on the CERN Linux platform. We have simulated one super module with 24 scintillator walls (baseline option).

For both plastic and liquid scintillator strips of 1×1 cm^2 or 1 by 2.6 cm^2 have been simulated. The plastic scintillator (polystyrene) is a mixture of C, H with a density of 1.032. The strips are coated with TiO_2 (density of 4.26). The coating thickness is 200 microns. A 500 μm aluminum foil is put around the 64 strips.

The liquid scintillator is a mixture of H, C and has a density of 0.86 (BC517 from BICRON). The liquid is into a polycarbonate cell (mixture of H, C and O). Its size is 300 μm and its density is 1.12. A 250 micron aluminum foil is put around the 64 strips.

The attenuation of the fibers is parameterized with a short attenuation length and a long attenuation length. The short WLS attenuation length is 1.2 m. For the long WLS attenuation length, we use 4 or 7 meters (blue or green photo-cathode). The "short" and "long" attenuation lengths have the same weight (0.5). There is a Poisson fluctuation of the number of photo-electrons at the end of each strip.

For the analysis, the wall is divided into bricks of 12.7 cm in the X direction and 10.16 cm in the Y direction. The gaps between bricks are : 0.2 cm in X and 0.4 cm in Y.

We have simulated DIS events in several channels :

- 10 000 $\tau \rightarrow \mu$
- 5 000 $\tau \rightarrow e$
- 5 000 $\tau \rightarrow h$
- 5 000 ν_μ CC
- 5 000 ν_μ NC

We have also simulated QE events in several channels :

- 5 000 $\tau \rightarrow \mu$
- 5 000 $\tau \rightarrow e$
- 5 000 $\tau \rightarrow \pi$
- 5 000 $\tau \rightarrow \rho$
- 5 000 ν_μ CC

All the studies and the comparisons are made in term of brick finding efficiency divided into wall finding efficiency times vertex finding with a barycentric algorithm. For the studies we assumed the following values for the oscillation parameters : $\sin^2 2\theta = 1$ and $\Delta m^2 = 3\ 10^{-3}$ eV^2.

The localization of the wall is done with a neural network, trained on ν_μ NC events. The same neural network is used to locate the wall in all cases. Table 1 shows the wall finding efficiency in all configurations, for different types of events.

TAB. 1: Wall finding efficiency for the configurations studied.

Events	plastic 1 × 1 cm^2 (%)	plastic 1 × 2.6cm^2 (%)	liquid 1 × 1 cm^2	liquid 1 × 2.6 cm^2 (%)
DIS ν_μ CC	99.1 ± 0.8	98.5 ± 1.1	97.9 ± 1.3	97.7 ± 1.3
DIS ν_μ NC	91.1 ± 2.5	91.4 ± 2.5	93.1 ± 2.2	92.4 ± 2.3
DIS $\tau \rightarrow \mu$	98.1 ± 1.2	98.7 ± 1.0	98.5 ± 1.2	98.1 ± 1.2
DIS $\tau \rightarrow e$	98.1 ± 1.7	98.3 ± 1.6	98.9 ± 1.3	98.3 ± 1.6
DIS $\tau \rightarrow h$	98.5 ± 1.6	98.9 ± 1.3	98.6 ± 1.5	98.8 ± 1.4
QE ν_μ CC	97.5 ± 0.9	97.4 ± 0.9	96.9 ± 0.9	95.9 ± 1.1
QE $\tau \rightarrow \mu$	99.1 ± 0.7	97.8 ± 0.9	97.6 ± 1.0	96.4 ± 1.2
QE $\tau \rightarrow e$	98.4 ± 0.8	97.8 ± 0.9	97.9 ± 0.9	98.3 ± 0.9
QE $\tau \rightarrow \pi$	95.5 ± 1.5	96.2 ± 1.3	95.2 ± 1.5	95.1 ± 1.5
QE $\tau \rightarrow \rho$	98.9 ± 0.7	98.6 ± 0.8	98.8 ± 0.8	99.0 ± 0.7

The wall finding efficiency is around 98% in all cases, appart from the case DIS ν_μ NC where it is $\sim 91\%$. We remind that the new generator including nuclear effects and increased back scattering is not yet used.

Once the interaction wall has been identified, a barycentric algorithm is used to locate the vertex. The division into bricks is used to determine if the fitted and the true vertex are in the same brick or not. We calculate the brick finding efficiency as the ratio of the events for which fitted and true vertex are in the same brick over the number of good events (not passing through a hole).

3 Plastic scintillator studies

The plastic scintillator has been simulated in two configurations : 1 × 1 cm^2 and 1 × 2.6 cm^2. We have studied the effect of the photo-cathode for the localization of the bricks. We have also simulated a photo-detector "trigger" in terms of a threshold for the number of photo-electrons accepted.

3.1 Proposal results

In this section, we remind you the results obtained for the several events in the proposal. The simulation was done with scintillator strips of 2.5 cm width, coated with 50 microns of "lucite". There was no aluminum foil in the simulation. The reconstruction was done with 6 photo-electrons at center. The long attenuation length was 4.8 meters and had a weight of 35%. The short attenuation was 1.2 meter and had a weight of 65%. Table 2 and figure 1 show the results obtained for the proposal.

TAB. 2: Brick finding efficiency obtained for the proposal. These numbers are mean efficiencies obtained with an unoscillated energy spectrum.

Events	wall finding efficiency (%)	brick finding efficiency (%)
DIS ν_μ CC	97.3	78.3
DIS ν_μ NC	94.4	66.7
DIS $\tau \rightarrow \mu$	96.4	74.6
DIS $\tau \rightarrow e$	97.4	81.8
DIS $\tau \rightarrow h$	95.9	77.3
QE ν_μ CC	95.4	81.7
QE $\tau \rightarrow \mu$	96.8	75.2
QE $\tau \rightarrow e$	98.2	83.9
QE $\tau \rightarrow \pi$	92.0	57.6
QE $\tau \rightarrow \rho$	97.2	80.0

3.2 Effect of the photo-cathode

To simulate two photo-cathodes ("green" or "blue") we have used two options for the reconstruction :

- 6 photo-electrons at center (that is 3 at each side) and a long attenuation length of 4 meters (results obtained on the full scale prototype build in Strasbourg with Pol.Hi.Tec scintillator plus 1 mm fiber),
- 9 photo-electrons at center and a long attenuation length of 6-7 meters (higher quantum efficiency and longer attenuation length).

In the two cases, the short attenuation length is the same (1.2 meter) and the two terms of attenuation have the same weight.

In table 3, we summarize the results for the two options. No cut is applied on the number of photo-electrons.

We find the same efficiency for the two cases. This is also what we can see on figure 2 for DIS $\tau \rightarrow \mu$ events and DIS $\tau \rightarrow h$ events, where the efficiency is plotted as a function of neutrino energy.

On figure 3 we can see the brick finding efficiency for the DIS and QE ν_μ CC events.

We further have used DIS $\tau \rightarrow \mu$ events in plastic scintillator strips (1×2.6 cm^2) to examine the effect on the brick finding efficiency of the number of photo-electrons. As can be seen on figure 4 we arrive at a plateau above 6 photo-electrons or more.

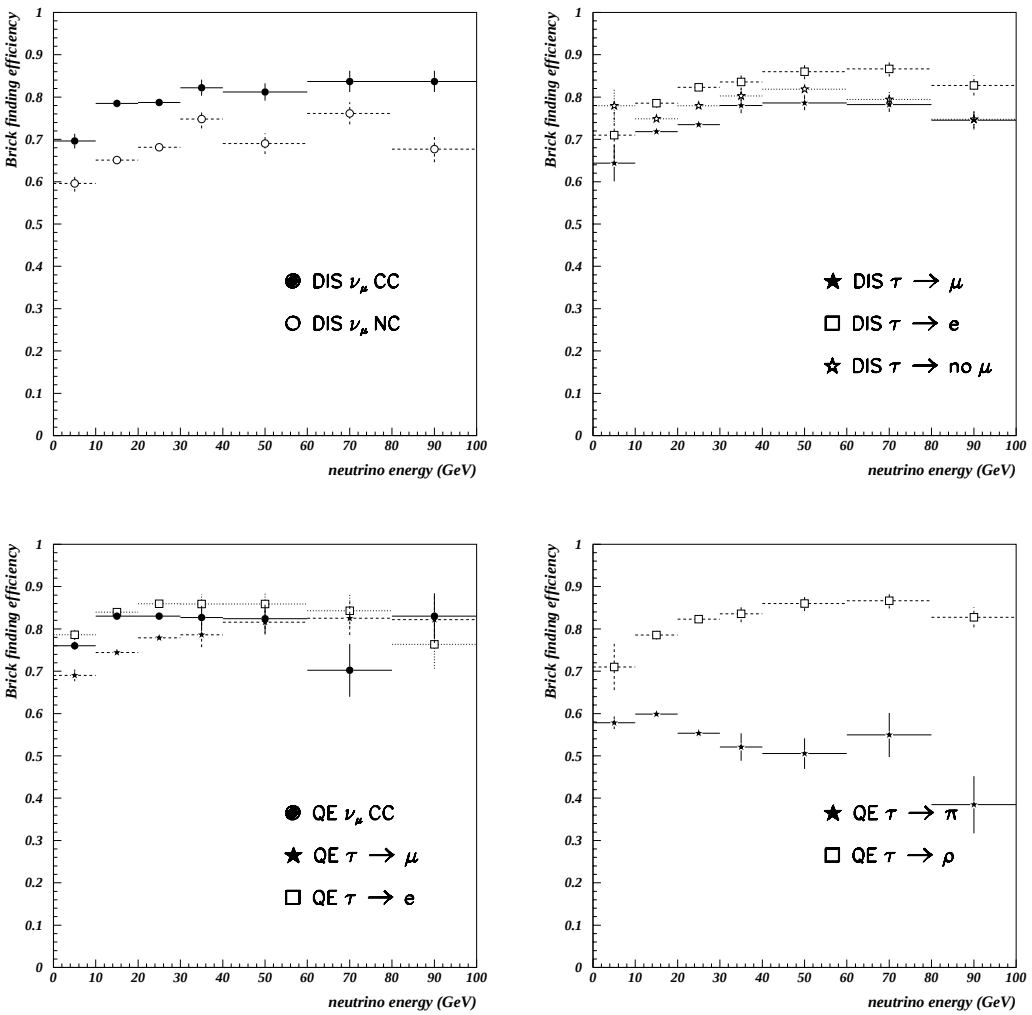

FIG. 1: Brick finding efficiency for several types of events, with the proposal configuration.

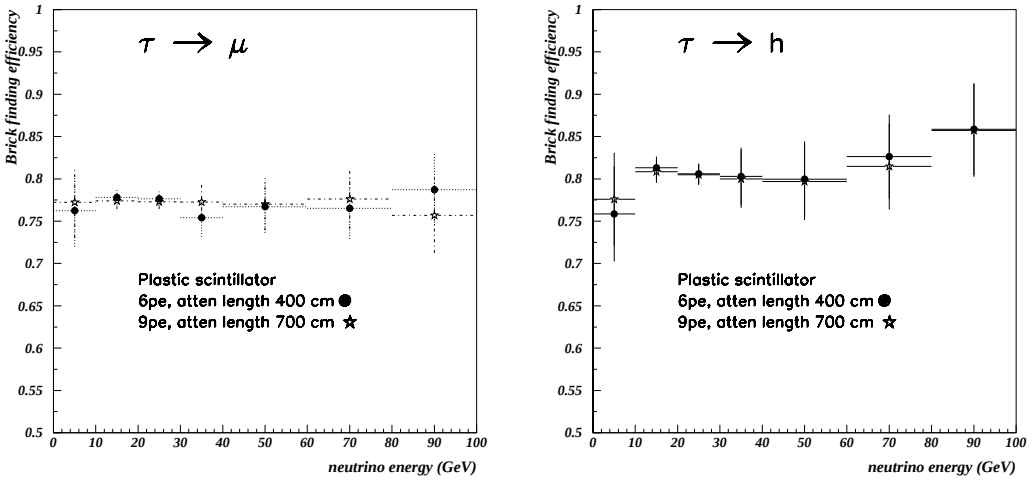

FIG. 2: Brick finding efficiency with 6 photo -electrons at center or 9 photo-electrons at center for DIS $\tau \to \mu$ events (left plot) and for DIS $\tau \to h$ events (right plot).

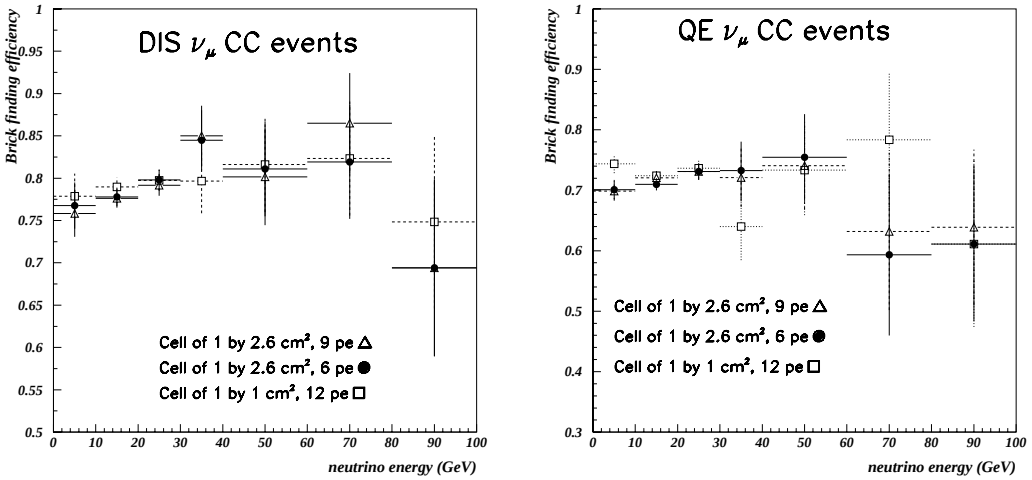

FIG. 3: Brick finding efficieny for DIS ν_μ CC events (left plot) and for QE ν_μ CC events (right plot).

TAB. 3: Brick finding efficiency with the two options for plastic scintillator strips of 1×2.6 cm^2.

Events	6 pe at center (%)	9 pe at center (%)
DIS ν_μ CC	78.9 ± 0.7	78.7 ± 0.97
DIS ν_μ NC	69.4 ± 0.7	70.1 ± 0.7
DIS $\tau \rightarrow \mu$	77.4 ± 3.7	76.8 ± 3.7
DIS $\tau \rightarrow e$	82.9 ± 4.5	83.7 ± 4.5
DIS $\tau \rightarrow h$	82.6 ± 4.9	82.5 ± 4.9
QE ν_μ CC	71.3 ± 0.7	71.7 ± 0.3
QE $\tau \rightarrow \mu$	73.1 ± 2.9	73.7 ± 2.9
QE $\tau \rightarrow e$	83.7 ± 2.4	83.7 ± 2.4
QE $\tau \rightarrow \pi$	67.2 ± 3.3	62.2 ± 3.3
QE $\tau \rightarrow \rho$	78.8 ± 2.9	78.6 ± 2.9

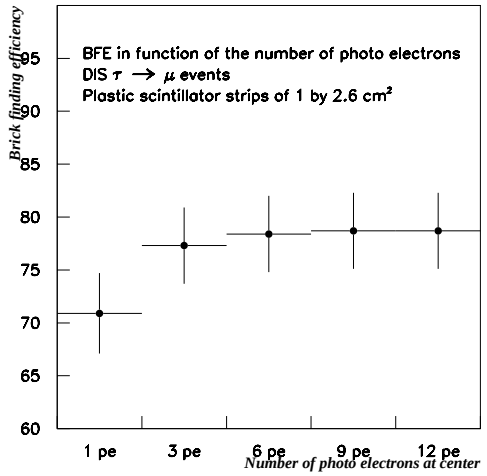

FIG. 4: Brick finding efficiency as a function of the number of photo-electrons at center. No thresholds were applied. We assume a maximal mixing angle and $\Delta m^2 = 3\ 10^{-3}$ eV^2.

3.3 Photo-detector "trigger"

We have simulated a threshold applied at the photo-detector level. The reconstruction is done with 3, 6, 9 or 12 photo-electrons at the center of the strips. The long attenuation length is 6 meters and the low attenuation length is 1.2 meter. The threshold is applied at both end (right and left) of each strip. We have used three thresholds :

- a threshold at ≥ 1 photo-electron,
- a threshold at ≥ 2 photo-electron,
- a threshold at ≥ 3 photo-electron.

The threshold is applied at the two ends of the strips. A strip is taken into account if both ends are higher than the threshold. The tables with the results are given in the appendix. The effect of these cuts are studied for all the events (DIS and QE) in plastic scintillator strips of 1×2.6 cm^2.

The effect of the cuts is around 6% with 6 photo-electrons and around 2% with 9 photo-electrons for DIS events. The effect is much more important for QE events, we have a diminution of efficiency larger than 10%. There is no effect for events with a shower, $\tau \to e$ and $\tau \to h$, but a large effect for event with single track.

Figure 5 shows the brick finding efficiency for the two last thresholds. These thresholds have a high effect on the brick finding efficiency.

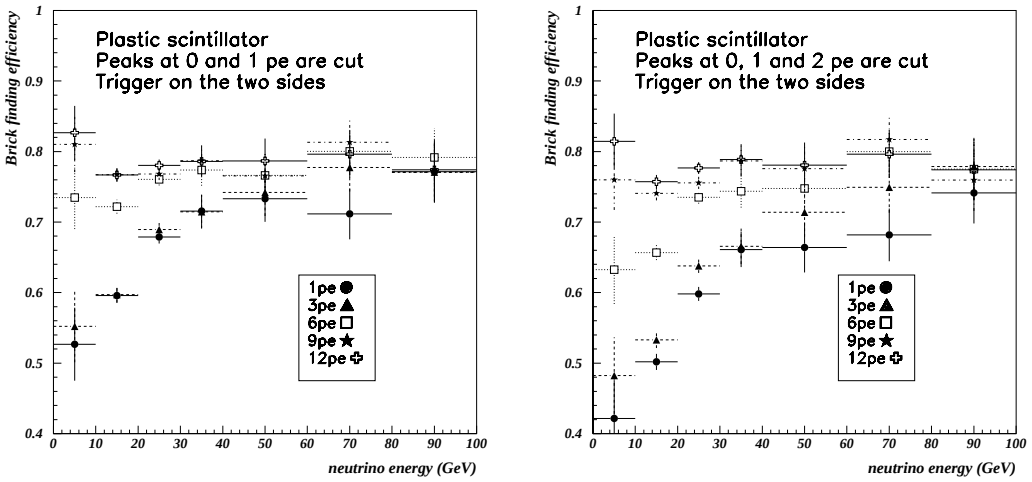

FIG. 5: Brick finding efficiency for the several options of trigger. The left plot shows the efficiency for a threshold at 2 photo-electrons on both ends and the right plot shows the efficiency for a threshold at 3 photo-electrons on both ends. These plots are done with DIS $\tau \to \mu$ events and plastic scintillator strips of 1×2.6 cm^2.

Another possibility, for the high (≥ 2 photo-electrons) threshold option, is to consider not the .AND. of the two sides but to consider a strip value even if only one end is higher than the threshold. The effect of this relaxed "trigger" is shown on table 4 for all the events and on figure 6 for DIS $\tau \to \mu$ events.

TAB. 4: Effect of a single side threshold ≥ 2 p.e. applied at the end of the strips on the brick finding efficiency w.r.t. the number of photo-electrons at the center of the strip. The values for the brick finding efficiency without cut are indicated into brackets.

events	3 pe (%)	6 pe (%)	9 pe (%)	12 pe
DIS ν_μ NC	67.2 (69.1)	69.2 (69.2)	69.7 (70.1)	69.5 (69.5)
DIS ν_μ CC	76.8 (78.5)	78.3 (78.4)	79.1 (78.7)	78.6 (79)
DIS $\tau \to \mu$	70.2 (77.3)	77.5 (78.4)	78.6 (78.7)	78.9 (78.7)
DIS $\tau \to e$	83.3 (83.7)	82.2 (84.2)	83.1 (83.3)	83.5 (83.9)
DIS $\tau \to h$	80.2 (82.0)	82.1 (83.8)	82.6 (82.9)	83.1 (82.9)
QE ν_μ CC	60.6 (68.4)	71.1 (71.5)	71.8 (71.8)	71.9 (72.5)
QE $\tau \to \mu$	67.7 (70.4)	72.2 (73.6)	73.5 (73.7)	74.1 (74.2)
QE $\tau \to e$	81.8 (82.5)	82.6 (83.6)	83.4 (83.7)	83.5 (83.1)
QE $\tau \to \pi$	59.3 (63.6)	66.4 (65.5)	66.8 (66.2)	66.7 (65.6)
QE $\tau \to \rho$	76.9 (77.7)	77.4 (78.8)	78.5 (78.6)	77.9 (78.4)

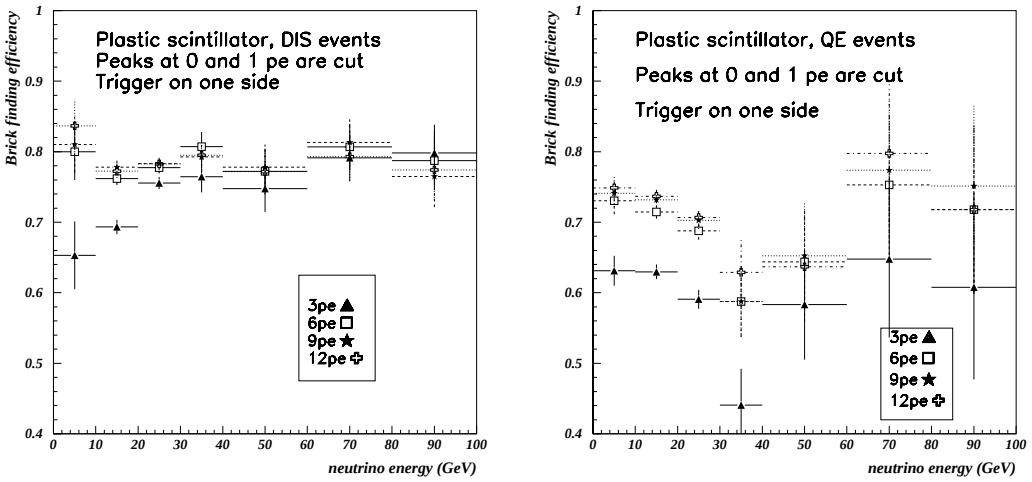

FIG. 6: Brick finding efficiency for a high threshold readout ($\geq$ 2 p.e.). At least one end is higher than the threshold. The left plot is done with DIS $\tau \rightarrow \mu$ events and the right plot is done with QE $\tau \rightarrow \mu$ events. For the two plots there are plastic scintillator strips of 1×2.6 cm^2.

This "relaxed" trigger gives a good stability for the brick finding efficiency for 6 photo-electrons or more.

3.4 Effect of the plastic scintillator strip size

The reconstruction for the cell of 1×1 cm^2 is done with :

– 12 photo-electrons plus 4 meters of attenuation length,

The reconstruction for the cell of 1×2.6 cm^2 is done with :

– 6 photo-electrons plus 4 meters of attenuation length,

– 9 photo-electrons plus 7 meters of attenuation length.

The factor 2 between the cells of 1×1 cm^2 and the cell of 1×2.6 cm^2 is a reasonable estimate.

The vertex resolution is calculated as the difference between the true vertex and the reconstructed vertex. This resolution is fitted by two gaussians. Figure 7 shows this resolution for ν_μ CC DIS events in the two configurations.

Figure 8 shows the vertex resolution for $\tau \rightarrow \mu$ QE events.

Tables 5 and 6 summarize the vertex resolution for all the events with the two configurations.

We can emphasize two effects for the vertex resolution :

– the resolution in Y is better than the resolution in X. This is due to the fact that the walls with Y strips are just behind the brick walls. The walls with X strips are after the wall with Y strips,

– the resolution for the strips of 1×1 cm^2 is better than the resolution for the strips of 1×2.6 cm^2. This improvement is varing between 0.2 cm to 1 cm for each gaussian.

Table 7 shows the comparison for the brick finding efficiency between the two cell sizes. The results show three effects :

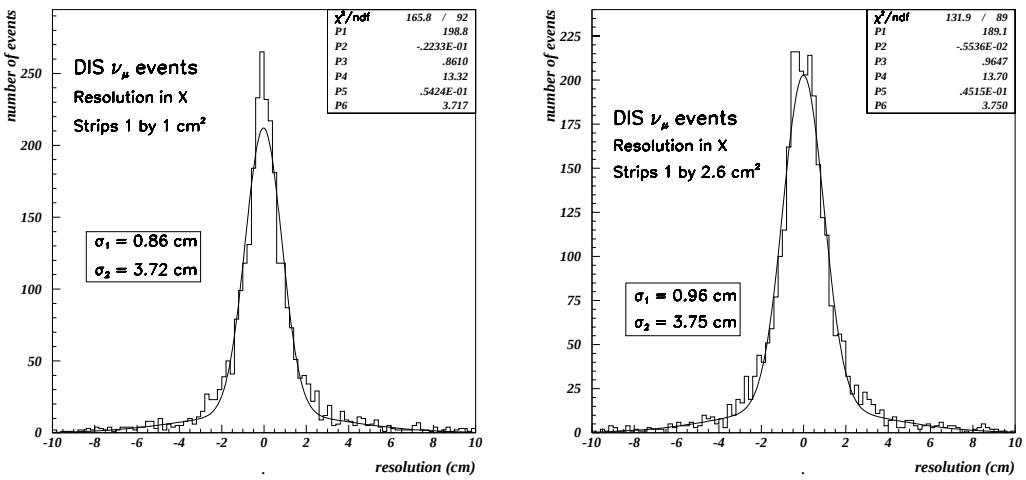

FIG. 7: Vertex resolution for ν_μ CC DIS events with plastic scintillator strips of 1×1 cm^2 (left plot) and with plastic scintillator strips of 1×2.6 cm^2 (right plot)

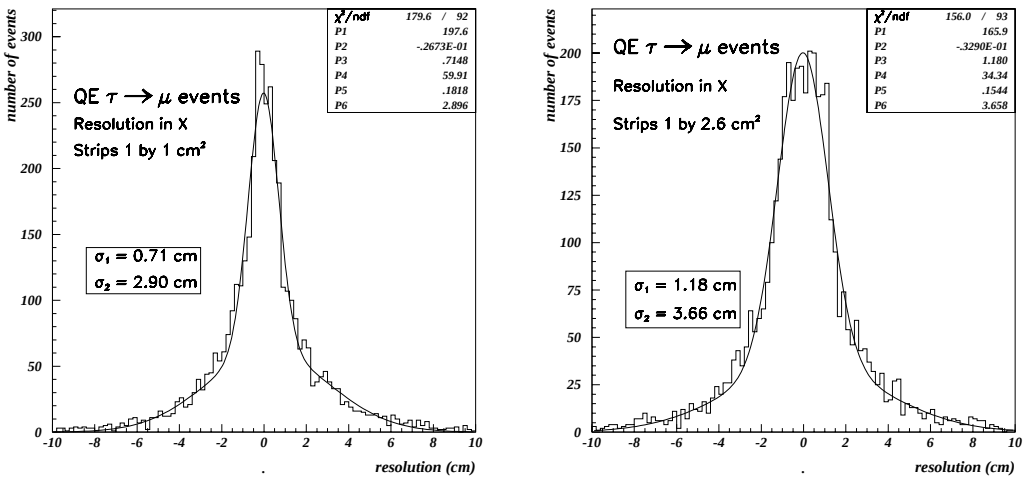

FIG. 8: Vertex resolution for $\tau \rightarrow \mu$ QE events with plastic scintillator strips of 1×1 cm^2 (left plot) and with plastic scintillator strips of 1×2.6 cm^2 (right plot)

TAB. 5: Vertex resolution in X for the two plastic scintillator strips size.

	1×1 cm^2 (12 pe)		1×2.6 cm^2 (6 pe)	
Events	σ_1 (cm)	σ_2 (cm)	σ_1 (cm)	σ_2 (cm)
DIS ν_μ CC	0.86 ± 0.04	3.72 ± 0.43	0.96 ± 0.03	3.75 ± 0.28
DIS ν_μ NC	0.93 ± 0.06	3.26 ± 0.28	0.86 ± 0.04	2.93 ± 0.13
DIS $\tau \to \mu$	0.82 ± 0.02	3.34 ± 0.16	0.92 ± 0.03	3.3 ± 0.18
DIS $\tau \to e$	0.61 ± 0.03	2.81 ± 0.37	0.72 ± 0.02	2.84 ± 2.90
DIS $\tau \to h$	0.63 ± 0.03	3.00 ± 0.20	0.72 ± 0.09	2.90 ± 1.20
QE ν_μ CC	0.45 ± 0.02	3.15 ± 0.91	0.99 ± 0.03	3.67 ± 0.13
QE $\tau \to \mu$	0.71 ± 0.05	2.90 ± 0.12	1.18 ± 0.07	3.66 ± 0.26
QE $\tau \to e$	0.57 ± 0.02	2.10 ± 0.13	0.72 ± 0.03	2.55 ± 0.27
QE $\tau \to \pi$	1.22 ± 0.08	3.66 ± 0.20	1.54 ± 0.19	4.08 ± 0.77
QE $\tau \to \rho$	0.69 ± 0.08	2.64 ± 0.81	0.81 ± 0.02	3.15 ± 0.21

TAB. 6: Vertex resolution in Y for the two plastic scintillator strips size.

	1×1 cm^2 (12 pe)		1×2.6 cm^2 (6 pe)	
Events	σ_1 (cm)	σ_2 (cm)	σ_1 (cm)	σ_2 (cm)
DIS ν_μ CC	0.51 ± 0.02	1.98 ± 0.11	0.79 ± 0.03	2.96 ± 0.30
DIS ν_μ NC	0.67 ± 0.03	2.87 ± 0.19	0.94 ± 0.04	3.73 ± 0.31
DIS $\tau \to \mu$	0.74 ± 0.02	3.37 ± 0.22	0.83 ± 0.02	2.74 ± 0.16
DIS $\tau \to e$	0.57 ± 0.01	2.73 ± 0.21	0.67 ± 0.02	2.72 ± 0.17
DIS $\tau \to h$	0.58 ± 0.02	2.73 ± 0.21	0.67 ± 0.02	2.72 ± 0.17
QE ν_μ CC	0.48 ± 0.02	2.70 ± 0.72	0.97 ± 0.03	3.21 ± 0.18
QE $\tau \to \mu$	0.62 ± 0.03	2.46 ± 0.10	1.17 ± 0.03	3.74 ± 0.21
QE $\tau \to e$	0.45 ± 0.02	1.64 ± 0.09	0.69 ± 0.18	2.47 ± 0.20
QE $\tau \to \pi$	1.11 ± 0.09	3.45 ± 0.30	1.27 ± 0.07	4.80 ± 0.25
QE $\tau \to \rho$	0.53 ± 0.02	2.31 ± 0.13	0.75 ± 0.02	2.76 ± 0.25

TAB. 7: Comparison of the brick finding efficiency for the two cell sizes.

Events	1×1 cm^2 (12 pe) (%)	1×2.6 cm^2 (6 pe) (%)
DIS ν_μ CC	79.3 ± 0.7	78.9 ± 0.7
DIS ν_μ NC	72.4 ± 0.7	69.4 ± 0.7
DIS $\tau \to \mu$	77.2 ± 3.7	77.4 ± 3.7
DIS $\tau \to e$	84.3 ± 4.5	82.9 ± 4.5
DIS $\tau \to h$	85.4 ± 4.6	82.6 ± 4.9
QE ν_μ CC	72.9 ± 0.7	71.3 ± 0.7
QE $\tau \to \mu$	77.0 ± 2.8	73.1 ± 2.9
QE $\tau \to e$	86.3 ± 2.3	83.7 ± 2.4
QE $\tau \to \pi$	68.7 ± 3.3	67.2 ± 3.3
QE $\tau \to \rho$	79.8 ± 2.8	78.8 ± 2.9

– the efficiency is slightly better for cells of 1×1 cm^2 than for cells of 1×2.6 cm^2 for the DIS ν_μ CC events (1%) and for the DIS $\tau \to h$ events (3%). We remind that no

muon tracking is included in the brick finding efficiency,

- there is no effect for the $\tau \rightarrow e$ events (due to the electro magnetic shower),
- for all the QE events, the cells of 1×1 cm^2 give a better brick finding efficiency than the cells of 1×2.6 cm^2.

Figure 9 shows the comparison between the two cell sizes for plastic scintillator and for DIS events.

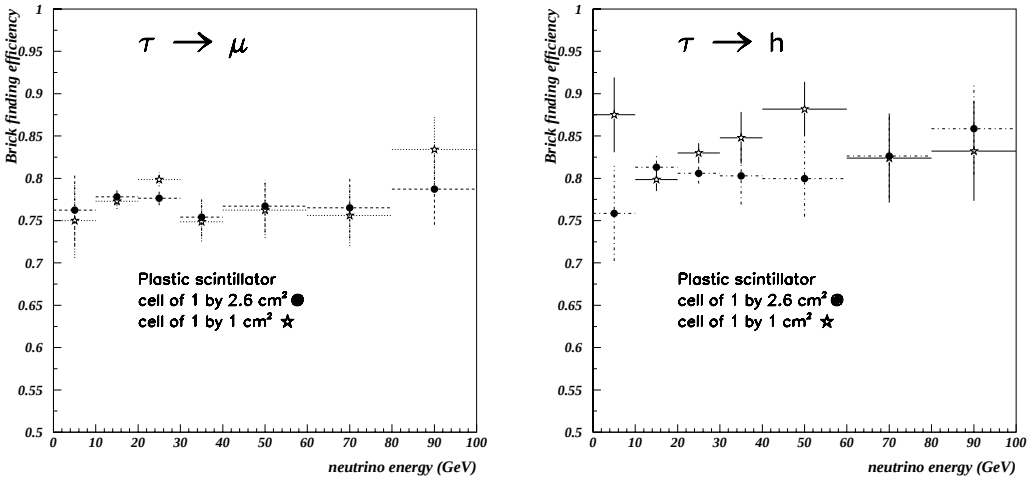

FIG. 9: Comparison of the brick finding efficiency for the two cell size of plastic scintillator strips for DIS $\tau \rightarrow \mu$ (left plot) and for DIS $\tau \rightarrow h$ (right plot).

Figure 10 shows the comparison between the two cell sizes for plastic scintillator and for QE events. We see that in all the cases and at low energy (≤ 30 GeV) the cells of 1×1 cm^2 give a better brick finding efficiency. Figure 3 shows this same effect for (DIS and QE) ν_μ events.

4 Liquid scintillator studies

The effect of the cell size is computed for the ten category of events. A simulation of optical cross talk has also been done.

4.1 Effect of the liquid scintillator strip size

For the cells of 1×1 cm^2 we generate 9 photo-electrons at the center and an attenuation length of 7 meters. These results have been obtained with a module of 3 planes of 4 liquid scintillator strips on a test with cosmic rays done in Lyon (see results presented by P. Jonsson during meeting at CERN in April 2001). For the cells of 1×2.6 cm^2 we put 4.5 photo-electrons at center. The scaling has been measured by I. Kreslo (presentation done during the meeting at CERN in April 2001).

In table 8 the brick finding efficiency for all the channels is summarized.

We have a better efficiency for cells of 1×1 cm^2 than for cells of 1×2.6 cm^2. This improvement is around 2% (figure 11 shows the comparison for DIS $\tau \rightarrow \mu$ events). For DIS

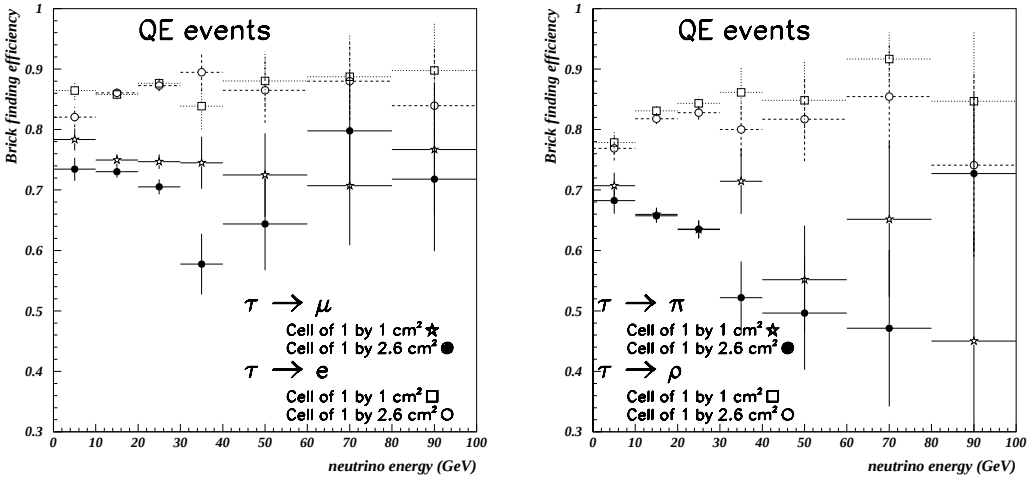

FIG. 10: Comparison of the brick finding efficiency for the two cell size of plastic scintillator strips for QE $\tau \to \mu$ (left plot) and for QE $\tau \to h$ (right plot).

TAB. 8: Brick finding efficiency for the two cell sizes with liquid scintillator.

Events	cell of 1×1 cm^2 (%)	cell of 1×2.6 cm^2 (%)
DIS ν_μ CC	78.6 ± 0.7	76.4 ± 0.7
DIS ν_μ NC	71.6 ± 0.7	71.3 ± 0.1
DIS $\tau \to \mu$	78.6 ± 3.7	76.4 ± 3.7
DIS $\tau \to e$	80.6 ± 4.9	81.4 ± 4.8
DIS $\tau \to h$	81.1 ± 5.2	79.8 ± 5.4
QE ν_μ CC	71.8 ± 0.7	69.7 ± 0.7
QE $\tau \to \mu$	75.5 ± 2.8	74.1 ± 2.8
QE $\tau \to e$	83.8 ± 2.4	86.2 ± 2.3
QE $\tau \to \pi$	65.1 ± 3.4	68.6 ± 3.3
QE $\tau \to \rho$	79.9 ± 2.8	80.7 ± 2.7

$\tau \to e$ events, there is no difference due to the presence of an electro-magnetic shower. This table is to be compared to table 7 for the plastic scintillator case.

4.2 Optical cross talk effect

The effect of optical cross talk was simulated. When a strip is hit, we put 10% of its energy on each neighboring strip, therefore we decrease its energy by 20%. Poisson fluctuation is then applied on each side of the strip. This study is done for cells of 1×1 cm^2 and for DIS $\tau \to \mu$ events.

In figure 12, we can see the resolution on the reconstructed vertex with and without cross talk. The resolution is slightly better with cross talk due to the barycentering.

This vertex resolution is converted into brick finding efficiency. Figure 13 shows this comparison. There is no difference between the two cases.

– 78.6 ± 3.7 % without cross talk

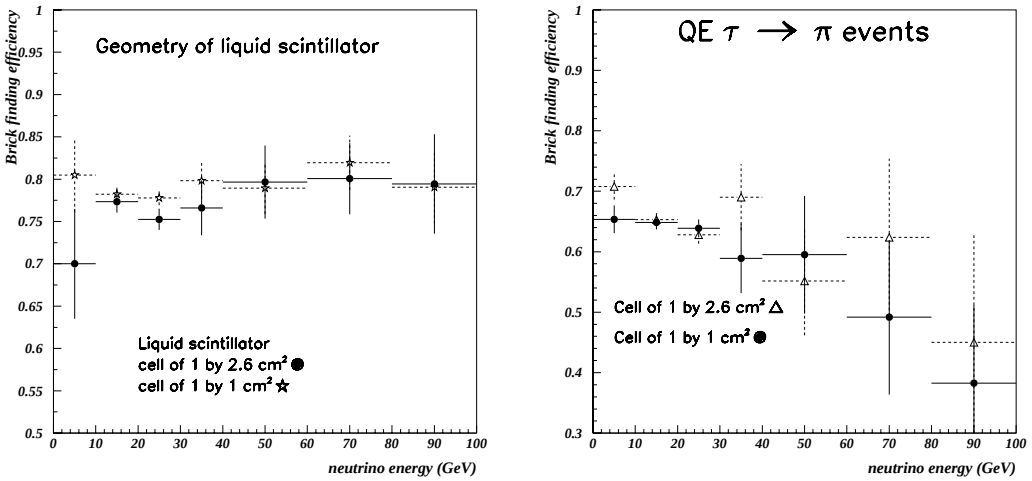

FIG. 11: Brick finding efficiency for DIS $\tau \to \mu$ (left plot) and for QE $\tau \to \pi$ (right plot) with the two liquid scintillator strips size.

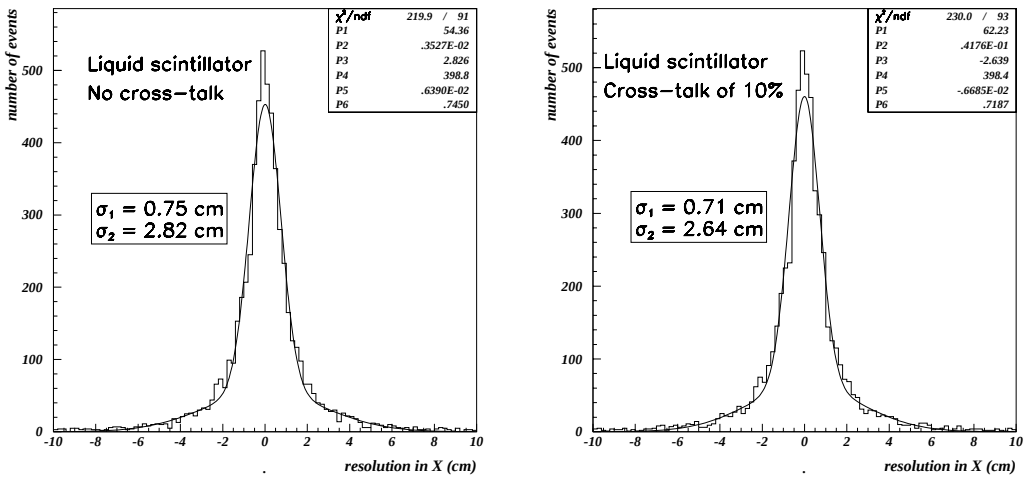

FIG. 12: Resolution for the reconstructed vertex without cross talk (left plot) and with 10% of cross talk (right plot) for DIS $\tau \to \mu$ events and 1×1 cm^2 liquid scintillator strips.

– 79.0 ± 3.6 % with 10% of cross talk

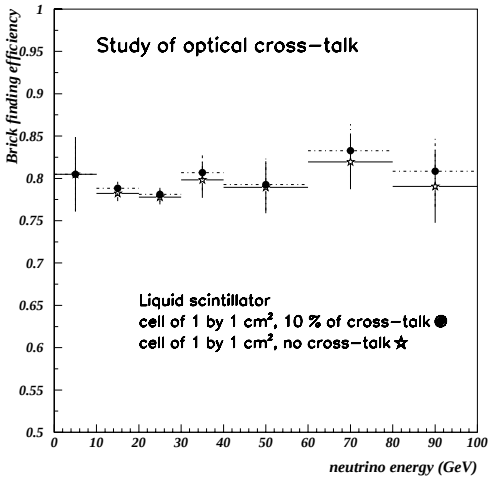

FIG. 13: Brick finding efficiency with and without cross talk for $\tau \rightarrow \mu$ events and 1×1 cm^2 liquid scintillator strips.

The optical cross talk is not a problem for the localization of the bricks. The latest measurements show a cross talk not higher than 3% (measurement done by I. Kreslo at CERN).

5 Two end readout versus one end readout and effects of the mirror characteristics

One option studied for the readout is a readout at only one end. Up to now, we have only studied the solution of a readout at both ends with a photo-detector on each side. This simulation is dedicated to the comparison between the two kinds of readout and also to the sensitivity of the mirror characteristics for the brick finding efficiency.

5.1 Comparison two end readout versus one end readout

In the one end readout we have put a mirror at the other extremity. The mirror has a reflectivity of 95%. We have tested two options for the readout ; 6 (respectively 9) photo-electrons at center and an attenuation length of 4 (respectively 7) meters. In figure 14 we can see the effect of a mirror when we have 6 photo-electrons or 9 photo-electrons. This study is realised with DIS $\tau \rightarrow \mu$ events and 1×2.6 cm^2 plastic scintillator strips.

There is a very small effect ($< 1\%$) between the two options when there are 9 photo-electrons at the center but a large effect ($> 4\%$) when there are only 6 photo-electrons at the center.

5.2 Impact of the reflectivity of the mirror

We have simulated a readout at one end with mirrors of varying reflectivity. This study is done with DIS $\tau \rightarrow \mu$ events with plastic scintillator strips of 1×2.6 cm^2 and without

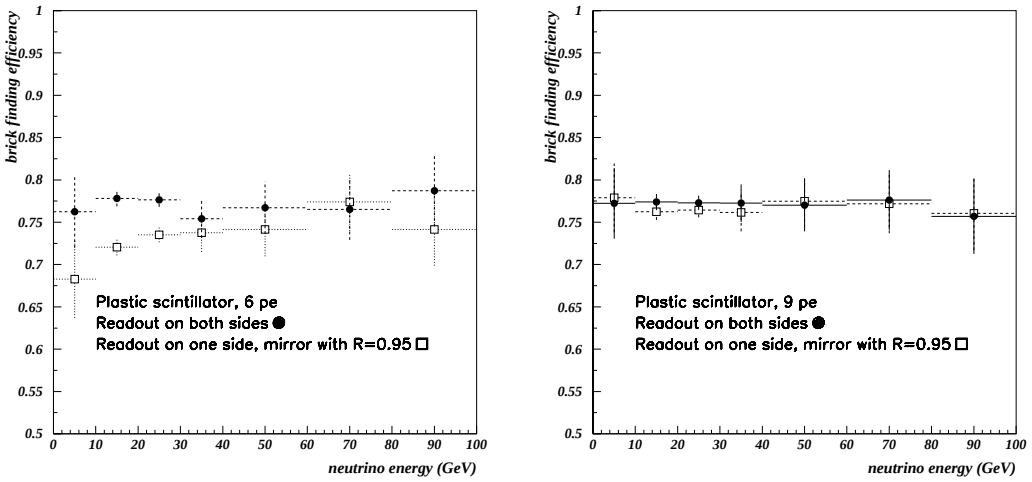

FIG. 14: Comparison between readout at one end and readout at two ends with 6 photo-electrons (left plot) and 9 photo-electrons (right plot) for DIS $\tau \to \mu$ events and 1×2.6 cm^2 plastic scintillator strips.

any threshold. The coefficient of reflectivity for the mirror is varied between 0.95 and 0.5. The effect of this variation is shown on figure 15.

We can underline two effects :

- for a one end readout, the brick finding efficiency is independent of the reflectivity of the mirror in the range 0.95 - 0.5. The main difference, when there is one, is between two ends versus one end readout,
- this difference is important when there are 6 photo-electrons at center but there is a very small effect ($< 1\%$) with 9 photo-electrons at center.

5.3 Effect of attenuation length

The longest attenuation length is an important parameter for the determination of the number of photo-electrons that can be seen. We varried this length between 2 and 11 meters. The other attenuation length ("the short attenuation") is kept at 1.2 meter. The two attenuations have the same weight. This study is done for DIS $\tau \to \mu$ events in plastic strips of 1×2.6 cm^2 with a mirror which coefficient of reflectivity is 0.7. The two cases, 6 or 9 photo-electrons have been simulated. In figure 16 we can see the evolution of the brick finding efficiency as a function of the attenuation length.

We can see that we reach a plateau for the brick finding efficiency for an attenuation length ~ 7 meters.

6 Effect of clear fiber

We have simulated the effect of clear fiber on the brick finding efficiency for DIS $\tau \to \mu$ events with 1×2.6 cm^2 plastic scintillator strips. For this purpose, we have used strips of 6.7 meters read by 6.7 meters WLS fibers. At the ends of the WLS fiber, we have added clear fibers. The length of these clear fibers is varying between 1.2 (mean value of the fibers with

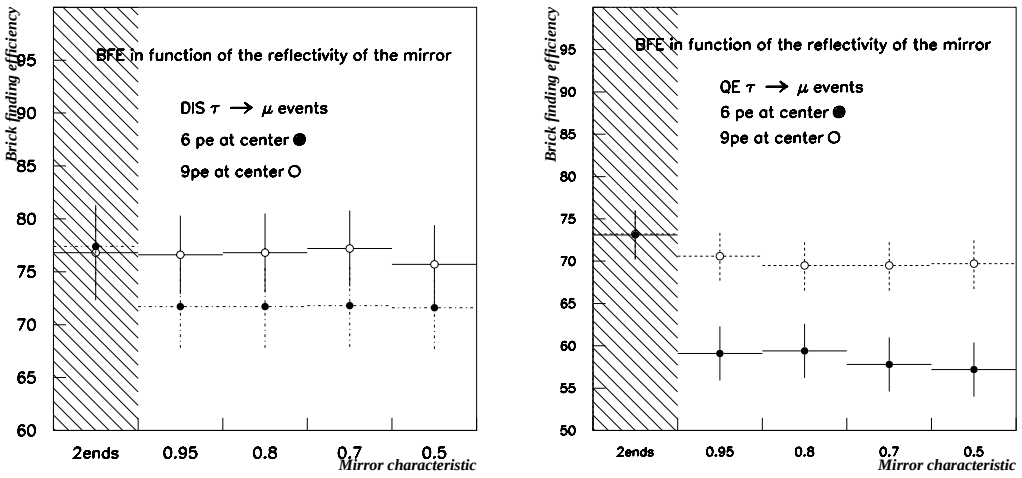

FIG. 15: Effect of the reflectivity of the mirror for the brick finding efficiency for DIS $\tau \rightarrow \mu$ events (left plot) and for QE $\tau \rightarrow \mu$ events (right plot). This studi is done with 1×2.6 cm^2 plastic scintillator strips.

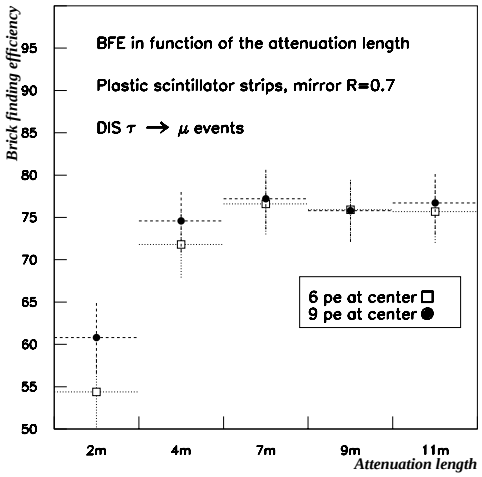

FIG. 16: Effect of the "long" attenuation length for the brick finding efficiency with 6 or 9 photo-electrons at center for DIS $\tau \rightarrow \mu$ events and 1×2.6 plastic scintillator strips.

two detectors by wall) to 4 meters (maximal value of the fibers with two detectors by wall). The transmission between the two fibers is assumed to be 90% and the attenuation length in the clear fiber is 10 meters (c.f. MINOS measurements : 12 meters, CDF : 10 meters). Poisson fluctuation is done at the end of the clear fibers.

In figure 17 we can see the effect of this clear fiber length on the brick finding efficiency. The length of the clear fiber has no effect for the localization of the bricks. There is also no difference between a 1 meter WLS fiber and a 1 meter clear fiber.

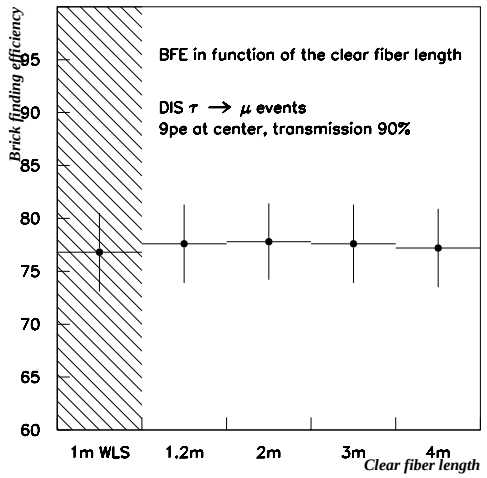

FIG. 17: Effect of a clear fiber for the brick finding efficiency for DIS $\tau \rightarrow \mu$ events and 1×2.6 plastic scintillator strips.

In figure 18 we can see the comparison between a one end readout with a mirror and a clear fiber, and a two end readout. The reflectivity of the mirror is 0.8. At the other end we have put 1.2 meter of clear fiber after the 6.7 meters of WLS fibers. The transmission between the two fibers is 90% and the attenuation length is 10 meters in the clear fiber. This comparison is done for DIS $\tau \rightarrow \mu$ events in plastic scintillator strips of 1×1 cm^2 with 15 photo-electrons at center and an attenuation length of 6 meters in the WLS fibers.

The brick finding efficiency are :

- $76.6 \pm 3.7\%$ for a readout at two end,
- $75.4 \pm 3.7\%$ for a readout at one end with a mirror and a clear fiber.

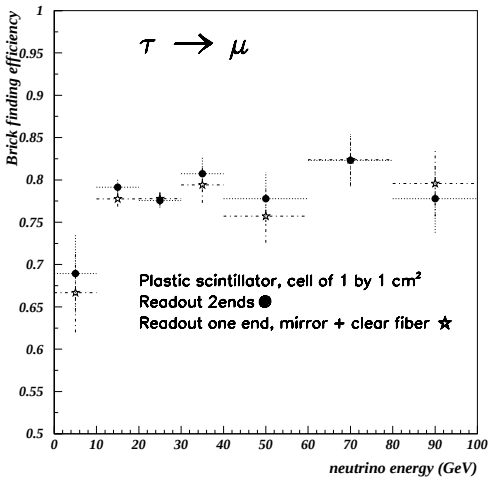

FIG. 18: Comparison between a readout at two end and a readout at one end with a mirror and an extra clear fiber for DIS $\tau \to \mu$ events and 1×1 cm^2 plastic scintillator strips.

7 Summary - Conclusions

The simulation of plastic and liquid scintillator strips for the target tracker has shown the following :

- the sensitivity to the size of the strip is very small. We have simulated cells of two size (1×1 cm^2 and 1×2.6 cm^2) for plastic and liquid scintillator, and the brick finding efficiency in the two cases is roughly the same. The smallest strips gives a higher brick finding efficiency by 3-4% for the events without shower and by 1% for events with shower. This differences may be increased by a retraining of the neural net or by including muon tracking,
- for the liquid scintillator, the optical cross talk (up to 10%) is not a problem for the localization of the bricks (the effect is lower than 0.5%),
- the effect of the photo-cathode sensitivity has been simulated for the two strip sizes. For the two photo-cathodes simulated, we have seen no effect for the brick finding efficiency,
- the threshold can be raised to ≥ 3 photo-electrons if we have at least 9 photo-electrons at the center of the strips,
- the effect of the readout at one end is negligible, around 1%, if we have at least 9 photo-electrons at center for the strips,
- the difference between a readout at two end and a readout at one end does not depend significantly on the reflectivity of the mirror,
- the attenuation length plays a central role for the readout at one end. We arrive at a plateau value for an attenuation length higher than 7 meters,
- an extra clear fiber of 2-4 meters with 90% transmission has no effect for the localization of the bricks.

The conclusions of this note will have to be reevaluated after the inclusion of muon tracking in the algorithm and a realistic back scattering generator.

Annex - Trigger tables

The following tables summarize the effect of the thresholds applied at the end of the strips on the brick finding efficiency w.r.t. the number of photo-electrons at the center of the strip. This study is done for plastic scintillator strips of 1×2.6 cm^2 and with a long attenuation length of 6 meters. All the results are obtained with $\Delta m^2 = 3\ 10^{-3}$ eV^2 and $\sin^2 2\theta$ =1.

TAB. 9: DIS ν_μ CC events.

cuts	3 pe (%)	6 pe (%)	9 pe (%)	12 pe
$\geq$ 1 p.e.	75.9 $\pm$ 0.7	78.5 $\pm$ 0.7	78.5 $\pm$ 0.7	78.9 $\pm$ 0.7
$\geq$ 2 p.e.	69.1 $\pm$ 0.7	76.3 $\pm$ 0.7	77.9 $\pm$ 0.7	78.7 $\pm$ 0.7
$\geq$ 3 p.e.	64.6 $\pm$ 0.7	73.2 $\pm$ 0.7	76.7 $\pm$ 0.7	78.2 $\pm$ 0.7

TAB. 10: DIS ν_μ NC events.

cuts	3 pe (%)	6 pe (%)	9 pe (%)	12 pe
$\geq$ 1 p.e.	66.1 $\pm$ 0.7	68.3 $\pm$ 0.7	70.3 $\pm$ 0.7	69.5 $\pm$ 0.7
$\geq$ 2 p.e.	61.5 $\pm$ 0.7	66.6 $\pm$ 0.7	69.8 $\pm$ 0.4	69.5 $\pm$ 0.7
$\geq$ 3 p.e.	58.9 $\pm$ 0.7	64.3 $\pm$ 0.7	67.9 $\pm$ 0.4	69.1 $\pm$ 0.7

TAB. 11: DIS $\tau \rightarrow \mu$ events.

cuts	3 pe (%)	6 pe (%)	9 pe (%)	12 pe
$\geq$ 1 p.e.	71.8 $\pm$ 3.9	77.6 $\pm$ 3.6	78.5 $\pm$ 3.6	78.5 $\pm$ 3.6
$\geq$ 2 p.e.	61.4 $\pm$ 4.3	73.5 $\pm$ 3.8	77.7 $\pm$ 3.6	78.3 $\pm$ 3.6
$\geq$ 3 p.e.	55.4 $\pm$ 4.5	67.3 $\pm$ 4.1	75.0 $\pm$ 3.8	77.4 $\pm$ 3.7

TAB. 12: DIS $\tau \rightarrow e$ events.

cuts	3 pe (%)	6 pe (%)	9 pe (%)	12 pe
$\geq$ 1 p.e.	83.4 $\pm$ 4.5	83.9 $\pm$ 4.5	83.2 $\pm$ 4.6	84.2 $\pm$ 4.4
$\geq$ 2 p.e.	80.8 $\pm$ 4.8	81.2 $\pm$ 4.8	82.9 $\pm$ 4.6	83.7 $\pm$ 4.4
$\geq$ 3 p.e.	79.4 $\pm$ 4.9	79.9 $\pm$ 4.9	82.4 $\pm$ 4.6	83.9 $\pm$ 4.5

TAB. 13: DIS $\tau \to h$ events.

cuts	3 pe (%)	6 pe (%)	9 pe (%)	12 pe
≥ 1 p.e.	81.8 ± 4.9	83.7 ± 4.7	83.1 ± 4.8	82.8 ± 4.9
≥ 2 p.e.	77.8 ± 5.3	83.2 ± 4.8	83.2 ± 4.8	83.0 ± 4.8
≥ 3 p.e.	73.6 ± 5.7	80.0 ± 5.1	82.8 ± 4.9	83.1 ± 4.8

TAB. 14: QE ν_μ CC events.

cuts	3 pe (%)	6 pe (%)	9 pe (%)	12 pe
≥ 1 p.e.	51.0 ± 0.7	63.9 ± 0.7	69.1 ± 0.7	71.7 ± 0.7
≥ 2 p.e.	31.8 ± 0.7	51.4 ± 0.7	62.2 ± 0.7	67.9 ± 0.7
≥ 3 p.e.	25.9 ± 0.7	38.8 ± 0.7	52.7 ± 0.7	60.8 ± 0.7

TAB. 15: QE $\tau \to \mu$ events.

cuts	3 pe (%)	6 pe (%)	9 pe (%)	12 pe
≥ 1 p.e.	54.1 ± 3.3	67.5 ± 3.0	71.6 ± 2.9	73.3 ± 2.9
≥ 2 p.e.	35.7 ± 3.2	55.4 ± 3.3	67.0 ± 3.1	70.1 ± 3.0
≥ 3 p.e.	28.8 ± 3.6	44.2 ± 3.3	57.9 ± 2.8	63.8 ± 3.1

TAB. 16: QE $\tau \to e$ events.

cuts	3 pe (%)	6 pe (%)	9 pe (%)	12 pe
≥ 1 p.e.	81.9 ± 2.5	83.3 ± 2.4	83.8 ± 2.4	83.1 ± 2.4
≥ 2 p.e.	79.1 ± 2.7	82.6 ± 2.5	83.2 ± 2.4	83.1 ± 2.4
≥ 3 p.e.	81.2 ± 2.6	83.5 ± 2.4	83.6 ± 2.4	83.3 ± 2.4

TAB. 17: QE $\tau \to \pi$ events.

cuts	3 pe (%)	6 pe (%)	9 pe (%)	12 pe
≥ 1 p.e.	50.8 ± 3.5	62.2 ± 3.4	65.0 ± 3.4	65.7 ± 3.3
≥ 2 p.e.	37.3 ± 3.5	54.6 ± 3.5	60.5 ± 3.4	63.9 ± 3.4
≥ 3 p.e.	29.9 ± 3.5	45.2 ± 3.6	53.9 ± 3.5	59.6 ± 3.5

TAB. 18: QE $\tau \to \rho$ events.

cuts	3 pe (%)	6 pe (%)	9 pe (%)	12 pe
≥ 1 p.e.	77.1 ± 2.1	78.6 ± 2.9	78.4 ± 2.9	78.2 ± 2.9
≥ 2 p.e.	75.0 ± 2.2	76.6 ± 3.0	77.7 ± 2.9	78.0 ± 2.9
≥ 3 p.e.	76.9 ± 2.2	74.8 ± 3.1	75.9 ± 3.0	77.9 ± 2.9